

Collapsible Linear Blocks for Super-Efficient Super Resolution

Kartikeya Bhardwaj¹, Milos Milosavljevic², Alex Chalfin¹, Naveen Suda¹,
Liam O’Neil^{3,*}, Dibakar Gope^{2,*}, Lingchuan Meng¹, Ramon Matas⁴, and Danny Loh¹
¹Arm Inc., San Jose, CA, USA, ²Arm Research, Austin, TX, USA
³Arm Inc., Cambridge, UK, ⁴Arm Research, Boston, MA, USA

kartikeya.bhardwaj@arm.com

Abstract

With the advent of smart devices that support 4K and 8K resolution, Single Image Super Resolution (SISR) has become an important computer vision problem. However, most super resolution deep networks are computationally very expensive. In this paper, we propose SESR, a new class of Super-Efficient Super Resolution networks that significantly improve image quality and reduce computational complexity. Detailed experiments across six benchmark datasets demonstrate that SESR achieves similar or better image quality than state-of-the-art models while requiring $2\times$ to $330\times$ fewer Multiply-Accumulate (MAC) operations. As a result, SESR can be used on constrained hardware to perform $\times 2$ (1080p to 4K) and $\times 4$ SISR (1080p to 8K). Towards this, we simulate hardware performance numbers for a commercial mobile Neural Processing Unit (NPU) for 1080p to 4K ($\times 2$) and 1080p to 8K ($\times 4$) SISR. Our results highlight the challenges faced by super resolution on AI accelerators and demonstrate that SESR is significantly faster than existing models. Overall, SESR establishes a new Pareto frontier on the quality (PSNR)-computation relationship for the super resolution task. The code for this work is available at <https://github.com/ARM-software/sesr>.

1. Introduction

Single Image Super Resolution (SISR) is the classic ill-posed computer vision problem which aims to generate a high-resolution image from a low-resolution input. Recently, SISR and related super-sampling techniques have found applications in real-time upscaling of content up to 4K resolution [34, 5]. Moreover, with the advent of AI accelerators such as Neural Processing Units (NPUs) in upcoming 4K displays, laptops, and TVs [3], AI-based upscaling of content to 4K resolution is now possible. Indeed, state-of-the-art SISR techniques are based on Convolutional Neural Networks (CNNs) which are computation-

*Equal Contribution

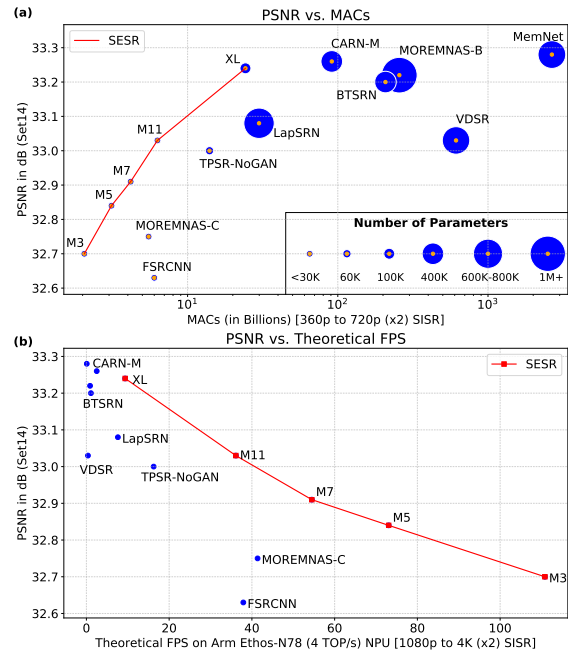


Figure 1. (a) PSNR on Set14 vs. MACs for different CNNs (360p to 720p, $\times 2$ SISR). (b) Most methods achieve less than 3FPS on a commercial Arm Ethos-N78 (4-TOP/s) mobile-NPU when performing 1080p to 4K SISR. SESR establishes a new Pareto frontier for image quality-computation relationship.

ally very expensive. Fig. 1(a) shows the quality, as measured by Peak Signal-to-Noise Ratio (PSNR), vs. a measure of computational complexity typically shown in SISR literature [1, 2, 20, 7], the number of Multiply-Accumulate (MAC) operations required to upscale an image from 360p to 720p. As evident, the existing models illustrate varied tradeoffs between image quality and computational costs.

To put the published figures in context, consider a more realistic scenario of 1080p to 4K upscaling on a commercial Arm Ethos-N78, 4-Tera Ops per second (4-TOP/s) mobile-NPU. This is an NPU suitable for deployment on a variety of mobile and smart devices such as smart phones, laptops, displays, TVs, etc. [3]. Fig. 1(b) shows the theo-

retical Frames Per Second (FPS) attained by various SISR networks. Clearly, even one of the smallest publicly available super resolution CNNs called FSRCNN [9] can theoretically (the best case, 100% hardware utilization scenario) achieve only 37 FPS on a 4-TOP/s NPU. When running on such constrained hardware, the larger deep networks are completely infeasible as most of them result in less than 3 FPS even in the best case. Hence, although many models like CARN-M [1] have been designed to be lightweight, most SISR networks *cannot* run on realistic, resource-constrained smart devices and mobile-NPUs. In addition, smaller models such as FSRCNN [9] or TPSR [20] do *not* achieve high image quality. Therefore, there is a need for significantly smaller and much more accurate CNNs that attain high throughputs on resource-constrained devices.

To this end, we propose a new class of super resolution networks called SESR that establish a new Pareto frontier on the quality-computation relationship (see Fig. 1(a)). Driven by our insight that the challenge of on-device SISR is one of model training as much as of model architecture, we introduce an innovation that modifies the training protocol without modifying the inference-time network architecture. Specifically, our models are based on *Collapsible Linear Blocks*, which are sequences of linear convolutional layers that can be analytically collapsed into single, narrow (in terms of input and channels) convolutional layers at inference time. We show that this modification of the training protocol, combined with new architectural features, results in Super-Efficient Super Resolution (SESR) networks that demonstrate state-of-the-art tradeoff between image quality and computational costs. Fig. 1(b) shows the theoretical FPS achieved by SESR on the Arm Ethos-N78 (4-TOP/s) NPU. Clearly, three out of five SESR CNNs theoretically achieve nearly 60 FPS or more when performing 1080p to 4K SISR.

Overall, we make the following **key contributions**:

1. We propose SESR, a new class of super-efficient super resolution networks that establish a new Pareto frontier on the quality-computation relationship. Towards this, we also propose Collapsible Linear Blocks as a way of training networks for significantly improved image quality and highly reduced computational complexity.
2. Our results clearly demonstrate the superiority of SESR over state-of-the-art models across six benchmark datasets for both $\times 2$ and $\times 4$ SISR. We achieve similar or better PSNR/SSIM than existing models while requiring $2\times$ to $330\times$ fewer MACs. Hence, SESR can be used on constrained hardware to perform $\times 2$ (1080p to 4K) and $\times 4$ SISR (1080p to 8K). We further provide concrete ablation studies to understand the effect of various design decisions in SESR.
3. Finally, we simulate hardware performance numbers

for a commercial Arm Ethos-N78 NPU using its performance estimator for 1080p to 4K ($\times 2$) and 1080p to 8K ($\times 4$) SISR. These results clearly show the real-world challenges faced by SISR on AI accelerators and demonstrate that SESR is substantially faster than existing models. We also discuss optimizations that eventually yield up to $8\times$ better runtime for 1080p to 4K SISR.

The rest of the paper is organized as follows: Section 2 discusses the related work, while Section 3 describes our proposed approach. Section 4 demonstrates the effectiveness of SESR over state-of-the-art CNNs, conducts ablation studies, and also simulates hardware performance for our proposed model. Finally, Section 5 concludes the paper.

2. Related Work

Numerous research efforts have been devoted to develop efficient super resolution networks using techniques based on compact network architecture design, neural architecture search (NAS), etc. SESR falls into the category of compact architecture design for resource-constrained devices.

Efficient SISR model design. While many excellent SISR methods have been proposed recently [16, 29, 36, 35], these works are difficult to deploy on resource-constrained devices due to their heavy computational complexity. To this end, FSRCNN [9] accelerates SISR by a compact network architecture. DRCN [17] and DRRN [28] adopt recursive layers to build deep network with fewer parameters. CARN [1], SplitSR [21], and GhostSR [24] reduce the compute complexity by combining lightweight residual blocks with variants of group convolution.

Other methods like [35, 22, 30, 23, 37] exploit attention mechanism to find the most informative region for reconstructing high-resolution image with better quality. Knowledge distillation [13] has also been leveraged to transfer the knowledge from big teacher networks to tiny student network [14]. In comparison, the SESR architecture exploits Collapsible Linear Blocks and residual connections which significantly improve the trainability and performance of our network without increasing the model complexity at inference time. Nevertheless, as different model compression techniques [1, 21, 24] are orthogonal to our compact network design, they can be used in conjunction with SESR to further reduce compute cost and model size.

Perceptual SISR networks. Another set of SISR methods innovate towards novel perceptual loss functions and Generative Adversarial Networks (GANs) [19, 31, 20]. These techniques result in photo-realistic image quality. However, since our primary goal is to improve compute-efficiency, we do not focus on such perceptual loss functions. We use the traditional losses like Mean Absolute Error in this work.

Linear overparameterization in deep networks. There has been limited but important research on linear overpa-

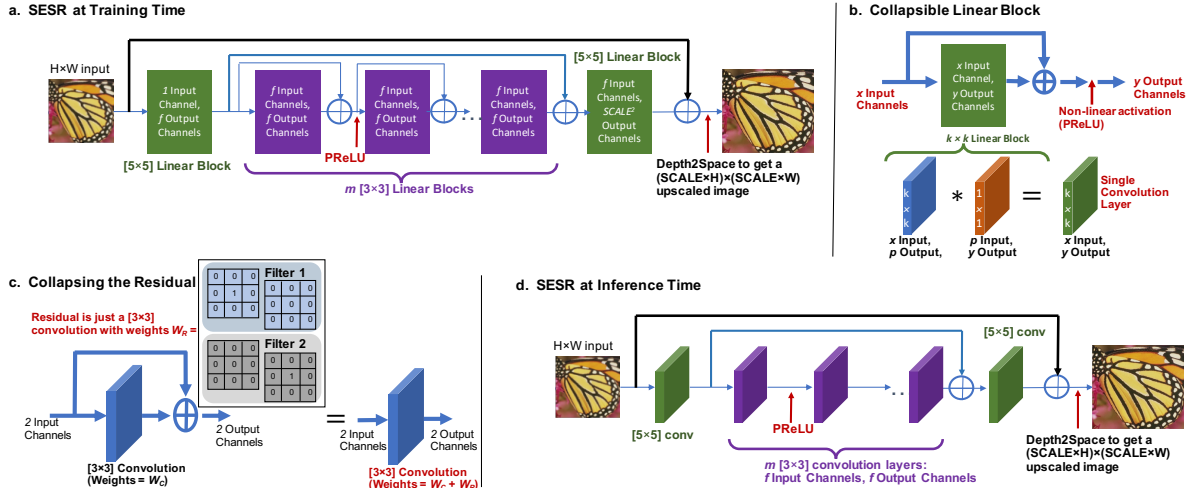


Figure 2. (a) Proposed SESR at training time contains two 5×5 and m 3×3 linear blocks. Two long residuals and several short residuals over 3×3 linear blocks exist. (b) A $k \times k$ linear block first uses a $k \times k$ convolution to project x input channels to p intermediate channels, which are projected back to y output channels via a 1×1 convolution. (c) Short residuals can further be collapsed into convolutions. (d) Final inference time SESR just contains two long residuals and $m+2$ narrow convolutions, resulting in super-efficient super resolution.

parameterization [4, 32, 8, 11] that shows the benefit of linearly overparameterized layers in speeding up the training of deep neural networks. Specifically, [4] theoretically demonstrates that the linear overparameterization of fully connected layers can accelerate the training of deep linear networks by acting as a time-varying momentum and adaptive learning rate. Recent work on ExpandNets [11] and ACNet [8] propose to overparameterize a convolutional layer and show that it accelerates the training of various CNNs and boosts the accuracy of the converged models. The kernel of a convolutional layer has both channel and spatial axes. While ExpandNets proposes to overparameterize a convolution kernel across the input and output channel axes, ACNet introduces an asymmetric convolution block, which essentially overparameterizes a convolution kernel across the center row and column of its spatial axes.

Our approach differs from existing linear overparameterization works [11, 8] in several ways: (i) Linear overparameterization blocks have not been proposed for the super resolution problem; (ii) We empirically demonstrate that existing linear overparameterization techniques like ExpandNets [11] are not effective for SISR tasks; (iii) To address this, we propose a new *Collapsible Linear Block* which combines overparameterization with residual connections. We further provide a procedure to collapse the residual analytically into the convolutions in order to reduce computational complexity of our models; (iv) Finally, existing work on linear overparameterization does not design entirely new networks but rather augments existing networks like MobileNets [25] with overparameterized layers. At inference time, the collapsed network is the same as the original MobileNet. On the other hand, SESR innovates in both the linear block design as well as the overall inference model

architecture to achieve state-of-the-art results for SISR.

NAS for lightweight super resolution. NAS techniques have been shown to outperform manually designed networks in many applications [38]. Therefore, recent works also attempt to apply NAS to super resolution tasks by exploiting lightweight convolutional blocks such as group convolution, inverted residual blocks with different channel counts and kernel sizes, dilations, residual connections, up-sampling layers, etc. [6, 12, 27, 33, 20]. While our focus is not on NAS, we demonstrate that SESR significantly outperforms state-of-the-art, NAS-designed SISR models.

3. Proposed Super-Efficient Super Resolution

In this section, we explain the SESR model architecture, collapsible linear blocks, and the inference SESR network.

3.1. SESR and Collapsible Linear Blocks

Fig. 2(a) illustrates SESR network at training time. As evident, SESR consists of multiple Collapsible Linear Blocks and several long and short residual connections. The structure of a linear block is shown in Fig. 2(b). Essentially, a $k \times k$ linear block with x input channels and y output channels first expands activations to p intermediate channels using a $k \times k$ convolution ($p \gg x$). Then, a 1×1 convolution is used to project the p intermediate channels to y final output channels. Since no non-linearity is used between these two convolutions, they can be *analytically* collapsed into a single narrow convolution layer at inference time, hence, the name Collapsible Linear Blocks. The final collapsed convolution has $k \times k$ kernel size while using only x input channels and y output channels. Therefore, at training time, we train a very large deep network which gets analytically collapsed into a highly efficient deep network

at inference time. This simple yet powerful overparameterization method, combined with residuals, shows significant benefits in convergence and image quality for SISR tasks.

We now describe the SESR model architecture in detail (see Fig. 2(a)). First, a 5×5 linear block is used to extract initial features from the input image. Next, the output of the first linear block passes through m 3×3 linear blocks with *short residuals*. Note that, a non-linearity (e.g., a Parametric ReLU or PReLU) is used after this short residual addition and not before (see Fig. 2(b)). The output of the first linear block is then added to the output of m 3×3 linear blocks (see *blue long-range residual* in Fig. 2(a)). Following this, we use another 5×5 linear block to output SCALE² channels. At this point, the input image is added back to all output activations (see *black long-range residual* in Fig. 2(a)). Finally, a *depth-to-space* operation converts the $H \times W \times \text{SCALE}^2$ activations into a $(\text{SCALE} \times H) \times (\text{SCALE} \times W)$ upscaled image. The depth-to-space operation described above is the same as the pixel shuffle part used inside subpixel convolutions [26, 20] and is one of the most standard techniques in SISR to obtain the upscaled images. Overall, our model is parameterized by $\{f, m\}$, where f represents the number of output channels at all the linear blocks except the last one, and m denotes the number of 3×3 linear blocks used in the SESR network.

Note that, a single $k \times k$ convolution decomposed into a large $k \times k$ and a 1×1 convolution was used in ExpandNets [11]. In Section 4.4, we empirically show that if a model just uses expanded convolutions without the short residuals (like in ExpandNets), it does not achieve good results for SISR tasks. Hence, short-residuals over the 3×3 linear blocks are essential for achieving good accuracy.

Collapsing the Linear Block. Once the SESR network is trained, we can collapse the linear blocks into single convolution layers. Algorithm 1 shows a detailed procedure to collapse the linear blocks which uses the following arguments: (i) Trained weights ($W_{1:L}$) for all layers within the linear block, (ii) Kernel Size (k) of linear block, (iii) #Input channels (N_{in}), and (iv) #Output channels (N_{out}). The output is the *analytically* collapsed weight W_C that replaces the linear block with a single small convolution layer.

Collapsing the Residual into Convolutions. Recall that, for our 3×3 linear blocks, we perform a non-linearity after the residual additions. This allows us to collapse the residuals into collapsed convolution weights W_C . Fig. 2(c) illustrates this process. Essentially, a residual is a 3×3 convolution with identity weights, *i.e.*, the output of this convolution is the same as its input. Fig. 2(c) shows what this weight looks like for a residual add with two input and output channels. Algorithm 2 shows a concrete pseudo code for collapsing the residual into a convolution. The final single convolution weight (combining both linear block and

Algorithm 1 Collapse Linear Block

```

1: procedure COLLAPSE_LB( $W_{1:L}, k, N_{in}, N_{out}$ )
2:   # First get NHWC tensor which will give the collapsed weight
3:    $\Delta \leftarrow \text{IDENTITY}(N_{in})$ 
4:    $\Delta \leftarrow \text{expand\_dim}(\text{expand\_dim}(\Delta, 1), 1)$ 
5:    $\Delta \leftarrow \text{ZERO\_PAD}(\Delta, [k-1, k-1])$ 
6:   for  $i = 1 : L$  do      ▷ Go through all layers in Linear Block
7:     if  $i == 1$  then
8:        $x \leftarrow \text{Conv2D}(\Delta, W_i)$ 
9:     else
10:       $x \leftarrow \text{Conv2D}(x, W_i)$ 
11:    end if
12:  end for
13:   $W_C \leftarrow \text{transpose}(\text{reverse}(x, [1, 2]), [1, 2, 0, 3])$ 
14:  return  $W_C$           ▷  $W_C$  is the collapsed weight
15: end procedure

```

Algorithm 2 Collapse Residual Addition into Convolution

```

1: procedure COLLAPSE_RESIDUAL( $W_C$ )
2:   shape  $\leftarrow W_C.\text{shape}$ 
3:   outChannels,  $k \leftarrow \text{shape}[3], \text{shape}[0]$ 
4:    $W_R \leftarrow \text{ZEROS}(\text{shape})$ 
5:   if  $k == 3$  then
6:     idx  $\leftarrow 1$ 
7:   end if
8:   if  $k == 5$  then
9:     idx  $\leftarrow 2$ 
10:  end if
11:  for  $i = 1 : \text{outChannels}$  do
12:     $W_R[\text{idx}, \text{idx}, i, i] \leftarrow 1$ 
13:  end for
14:  return  $W_R$           ▷  $W_R$  is the residual weight
15: end procedure

```

residual) is then given by $W_{3 \times 3} = W_C + W_R$.

3.2. SESR at Inference Time

The final, inference time SESR network architecture is shown in Fig. 2(d). As evident, all linear blocks and short residuals are collapsed into single convolutions. Hence, the final inference network is very simple: Just $m + 2$ convolution layers with most having f output channels, and two additional long residuals (see blue and black residuals in Fig. 2(d)). For this network, #parameters for $\times 2$ SISR is given by $P = (5 \times 5 \times 1 \times f) + m \times (3 \times 3 \times f \times f) + (5 \times 5 \times f \times 4)$ ¹. Then, #MACs can be calculated as #MACs = $H \times W \times P$, where H, W are the dimensions of the low resolution input. We obtain the best PSNR results using the network in Fig. 2(d). However, to achieve even better hardware efficiency, we create another version of SESR that removes the long black residual and replaces PReLU with

¹Following standard practice [9], we convert the RGB image into Y-Cb-Cr and use only the Y-channel for super resolution. This is why, there is only one input channel and one output channel for SESR.

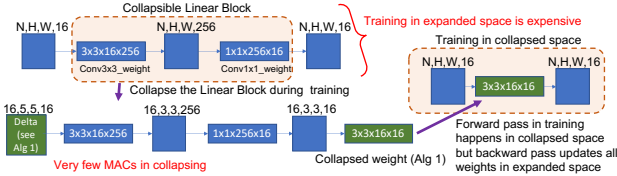


Figure 3. Collapsing (while training) is very efficient since the image size is 5×5 and batch size (N) is 16. These are much smaller than N, H, W when training in expanded space (i.e., $N=32$, image size is $H \times W = 64 \times 64$). Example: in expanded space, we have 32,64,64,256 tensors on which last 1×1 conv operates. In our efficient implementation, 1×1 conv operates on 16,3,3,256 tensor.

ReLU. We found that this does not have a significant impact on image quality (detailed ablations in next section).

3.3. Efficient Training Methodology

The training time would increase if we directly train collapsible linear blocks in the expanded space and collapse them later. To address this, we developed an efficient implementation of SESR: We collapse the Linear Blocks at each training step (using Algorithms 1 and 2), and then use this collapsed weight to perform forward pass convolutions. Since model weights are very small tensors compared to feature maps, this collapsing takes a very small time. *The training (backward pass) still updates the weights in the expanded space but the forward pass happens in collapsed space even during training* (see Fig. 3). Therefore, training the collapsible linear blocks is very efficient.

For the SESR-M5 network and a batch of 32 $[64 \times 64]$ images, training in expanded space takes 41.77B MACs for a single forward pass, whereas our efficient implementation takes only 1.84B MACs. Similar improvements happen in GPU memory and backward pass (due to reduced size of layerwise Jacobians). Therefore, training SESR networks is highly efficient.

4. Experimental Setup and Results

We first describe our setup, quantitative and qualitative results for SESR on six datasets. We then perform ablations to understand the effect of various optimizations in SESR. Finally, we simulate hardware performance for 1080p to 4K ($\times 2$) and 1080p to 8K ($\times 4$) SISR on Arm Ethos-N78 NPU.

4.1. Experimental Setup

We train our SESR networks for 300 epochs using ADAM optimizer with a constant learning rate of 5×10^{-4} and a batch size of 32 on DIV2K training set. We use mean absolute error (l_1) loss between the high resolution and generated images to train SESR. For training efficiency, we take 64 random crops of size 64×64 from each image; hence, each epoch conducts $800 \times 64/32 = 1600$ training steps. We vary the number of 3×3 linear blocks (m) as

$\{3, 5, 7, 11\}$ and keep number of channels as $f = 16$. We also train an extra-large model for SESR (called SESR-XL), where $f = 32$ and $m = 11$. Also, we set the expanded number of channels within linear blocks (parameter p in Fig. 2(b)) as 256. Once the training is complete, the models are collapsed using Algorithms 1, 2 and are tested on six standard SISR datasets: Set5, Set14, BSD100, Urban100, Manga109, and DIV2K validation set. Following standard practice, only Y-channel is used to compute PSNR/SSIM.

For $\times 4$ SISR, we start with the pretrained $\times 2$ SESR networks. We first replace the final $5 \times 5 \times f \times 4$ layer by $5 \times 5 \times f \times 16$ and then perform the depth-to-space operation twice. Note that, this is different from many prior SISR networks which repeat the upsampling block (containing a convolution *and* a depth-to-space operation) multiple times [20]. In contrast, we do a single convolution and apply depth-to-space twice. This helps us save additional MACs for $\times 4$ SISR. We will elaborate on this in the Results section. SESR is implemented in TensorFlow and the training is performed on a single NVIDIA V100 GPU.

4.2. Quantitative Results

Table 1 reports PSNR/SSIM for several networks on six datasets for $\times 2$ SISR. For clarity, we have broken down the results into three regimes: (i) Small networks with 25K parameters or less, (ii) Medium networks with 25K-100K parameters, and (iii) Large networks with more than 100K parameters. As evident, SESR dominates in all three regimes. Specifically, in the small network category, SESR-M5 achieves significantly better PSNR/SSIM than FSR-CNN [9] while using a similar number of parameters (e.g., 13.52K vs. 12.46K) and $\sim 2 \times$ fewer MACs (3.11G vs. 6.00G). Even our smallest CNN (SESR-M3) outperforms all prior models while using $2.6 \times$ to $3 \times$ fewer MACs.

In the medium network regime, we compare against the most recent tiny super resolution network called TPSR [20]. Note that, we have reported results for the TPSR-NoGAN setting since we have not focused on Generative Adversarial Networks (GANs) or any perceptual losses in this work. Clearly, SESR-M11 outperforms TPSR-NoGAN while requiring $2.2 \times$ fewer parameters and MACs. Note that, some of the baselines such as TPSR-NoGAN [20] and MOREMNAS [7] were found using advanced Neural Architecture Search (NAS) techniques and our (manually designed) SESR still significantly outperforms them.

For the large network category, we clearly see that our SESR-XL network either beats or comes close to much larger and highly accurate networks like CARN-M [1] (SESR uses $3.75 \times$ fewer MACs) and BTSRN [10] (SESR uses $8.55 \times$ fewer MACs). Most interestingly, our medium-range network (SESR-M11) actually achieves very similar or better PSNR than the VDSR network [15], which has $97 \times$ more MACs than SESR-M11.

Table 1. PSNR/SSIM results on $\times 2$ Super Resolution on several benchmark datasets. MACs are reported as the number of multiply-adds needed to convert an image to 720p (1280×720) resolution via $\times 2$ SISR. Red/Blue indicate Best/Second Best within each regime.

Regime	Model	Parameters	MACs	Set5	Set14	BSD100	Urban100	Manga109	DIV2K
Small	Bicubic	–	–	33.68/0.9307	30.24/0.8693	29.56/0.8439	26.88/0.8408	30.82/0.9349	32.45/0.9043
	FSRCNN (our setup)	12.46K	6.00G	36.85/0.9561	32.47/0.9076	31.37/0.8891	29.43/0.8963	35.81/0.9689	34.73/0.9349
	FSRCNN [9]	12.46K	6.00G	36.98/0.9556	32.62/0.9087	31.50/0.8904	29.85/0.9009	36.62/0.9710	34.74/0.9340
	MOREMNAS-C [7]	25K	5.5G	37.06/0.9561	32.75/0.9094	31.50/0.8904	29.92/0.9023	–/–	–/–
	SESR-M3 ($f=16, m=3$)	8.91K	2.05G	37.21/0.9577	32.70/0.9100	31.56/0.8920	29.92/0.9034	36.47/0.9717	35.03/0.9373
	SESR-M5 ($f=16, m=5$)	13.52K	3.11G	37.39/0.9585	32.84/0.9115	31.70/0.8938	30.33/0.9087	37.07/0.9734	35.24/0.9389
	SESR-M7 ($f=16, m=7$)	18.12K	4.17G	37.47/0.9588	32.91/0.9118	31.77/0.8946	30.49/0.9105	37.14/0.9738	35.32/0.9395
Medium	TPSR-NoGAN [20]	60K	14.0G	37.38/0.9583	33.00/0.9123	31.75/0.8942	30.61/0.9119	–/–	–/–
	SESR-M11 ($f=16, m=11$)	27.34K	6.30G	37.58/0.9593	33.03/0.9128	31.85/0.8956	30.72/0.9136	37.40/0.9746	35.45/0.9404
Large	VDSR [15]	665K	612.6G	37.53/0.9587	33.05/0.9127	31.90/0.8960	30.77/0.9141	37.16/0.9740	35.43/0.9410
	LapSRN [18]	813K	29.9G	37.52/0.9590	33.08/0.9130	31.80/0.8950	30.41/0.9100	37.53/0.9740	35.31/0.9400
	BTSRN [10]	410K	207.7G	37.75/–	33.20/–	32.05/–	31.63/–	–/–	–/–
	CARN-M [1]	412K	91.2G	37.53/0.9583	33.26/0.9141	31.92/0.8960	31.23/0.9193	–/–	–/–
	MOREMNAS-B [7]	1118K	256.9G	37.58/0.9584	33.22/0.9135	31.91/0.8959	31.14/0.9175	–/–	–/–
	SESR-XL ($f=32, m=11$)	105.37K	24.27G	37.77/0.9601	33.24/0.9145	31.99/0.8976	31.16/0.9184	38.01/0.9759	35.67/0.9420

Table 2. PSNR/SSIM results on $\times 4$ Super Resolution on several benchmark datasets. MACs are reported as the number of multiply-adds needed to convert an image to 720p (1280×720) resolution via $\times 4$ SISR. Red/Blue indicate Best/Second Best within each regime.

Regime	Model	Parameters	MACs	Set5	Set14	BSD100	Urban100	Manga109	DIV2K
Small	Bicubic	–	–	28.43/0.8113	26.00/0.7025	25.96/0.6682	23.14/0.6577	24.90/0.7855	28.10/0.7745
	FSRCNN (our setup)	12.46K	4.63G	30.45/0.8648	27.44/0.7528	26.89/0.7124	24.39/0.7212	27.40/0.8539	29.37/0.8117
	FSRCNN [9]	12.46K	4.63G	30.70/0.8657	27.59/0.7535	26.96/0.7128	24.60/0.7258	27.89/0.8590	29.36/0.8110
	SESR-M3 ($f=16, m=3$)	13.71K	0.79G	30.75/0.8714	27.62/0.7579	27.00/0.7166	24.61/0.7304	27.90/0.8644	29.52/0.8155
	SESR-M5 ($f=16, m=5$)	18.32K	1.05G	30.99/0.8764	27.81/0.7624	27.11/0.7199	24.80/0.7389	28.29/0.8734	29.65/0.8189
	SESR-M7 ($f=16, m=7$)	22.92K	1.32G	31.14/0.8787	27.88/0.7641	27.13/0.7209	24.90/0.7436	28.53/0.8778	29.72/0.8204
Medium	TPSR-NoGAN [20]	61K	3.6G	31.10/0.8779	27.95/0.7663	27.15/0.7214	24.97/0.7456	–/–	–/–
	SESR-M11 ($f=16, m=11$)	32.14K	1.85G	31.27/0.8810	27.94/0.7660	27.20/0.7225	25.00/0.7466	28.73/0.8815	29.81/0.8221
Large	VDSR [15]	665K	612.6G	31.35/0.8838	28.02/0.7678	27.29/0.7252	25.18/0.7525	28.82/0.8860	29.82/0.8240
	LapSRN [18]	813K	149.4G	31.54/0.8850	28.19/0.7720	27.32/0.7280	25.21/0.7560	29.09/0.8900	29.88/0.8250
	BTSRN [10]	410K	165.2G	31.85/–	28.20/–	27.47/–	25.74/–	–/–	–/–
	CARN-M [1]	412K	32.5G	31.92/0.8903	28.42/0.7762	27.44/0.7304	25.62/0.7694	–/–	–/–
	SESR-XL ($f=32, m=11$)	114.97K	6.62G	31.54/0.8866	28.12/0.7712	27.31/0.7277	25.31/0.7604	29.04/0.8901	29.94/0.8266

Similar results are obtained for $\times 4$ SISR. Recall that, we did not add multiple convolution layers in the upsampling block for SESR. This leads to even bigger savings in MACs for our proposed network. Table 2 shows the results for small, medium, and large categories. SESR-M5 now achieves better PSNR/SSIM than FSRCNN [9] with $4.4\times$ fewer MACs. In the medium regime, SESR-M11 either outperforms or comes very close to TPSR-NoGAN [20] while needing nearly $2\times$ fewer MACs. In the large network category, SESR-XL achieves similar or better image quality than LapSRN [18] while using $22.5\times$ fewer MACs. Finally, PSNR/SSIM of SESR-M11, again, comes very close to VDSR [15]. SESR-M11 requires $331\times$ fewer MACs than VDSR. As a result, our SESR-M11 network achieves VDSR-level performance even though it has nearly the same number of MACs as FSRCNN for $\times 2$ SISR and has $2.5\times$ fewer MACs than FSRCNN for $\times 4$ SISR. Hence, SESR significantly outperforms several state-of-the-art CNNs in image quality and computational costs.

For $\times 4$ SISR (large regime), there is still room for improvement. For instance, SESR-XL is nearly 0.4dB away from large CNNs like CARN-M [1] and BTSRN [10] for datasets like Urban100. This gap can potentially be filled

using more number of channels (f) or extra upsampling convolutions like in prior art. This is left as a future work.

4.3. Qualitative Evaluation

Fig. 4 and Fig. 5 show the image quality of various CNNs on $\times 2$ and $\times 4$ SISR, respectively. Since our focus is explicitly on highly efficient networks, we have compared the image quality of small- or medium-regime SESR against other small networks like FSRCNN [9]². As a reference for other high-quality models, we have provided the image for SESR-XL. Clearly, SESR-M5 outperforms FSRCNN (e.g., significantly sharper edges and less unwanted halo). SESR-M11 network performs even better than FSRCNN in all cases. Same holds for SESR-XL network. More qualitative results for $\times 2$ and $\times 4$ SISR are shown in Appendix A (see Fig. 6, Fig. 7). Therefore, SESR achieves significantly better image quality than other CNNs in similar compute regime.

4.4. Ablation Studies

In this section, we demonstrate the impact of various design decisions in SESR. We mainly modify the SESR-M11 network to conduct various ablation studies.

²Medium range SESR is considered here because it needs either similar (for $\times 2$ SISR) or even fewer (for $\times 4$ SISR) MACs than FSRCNN.

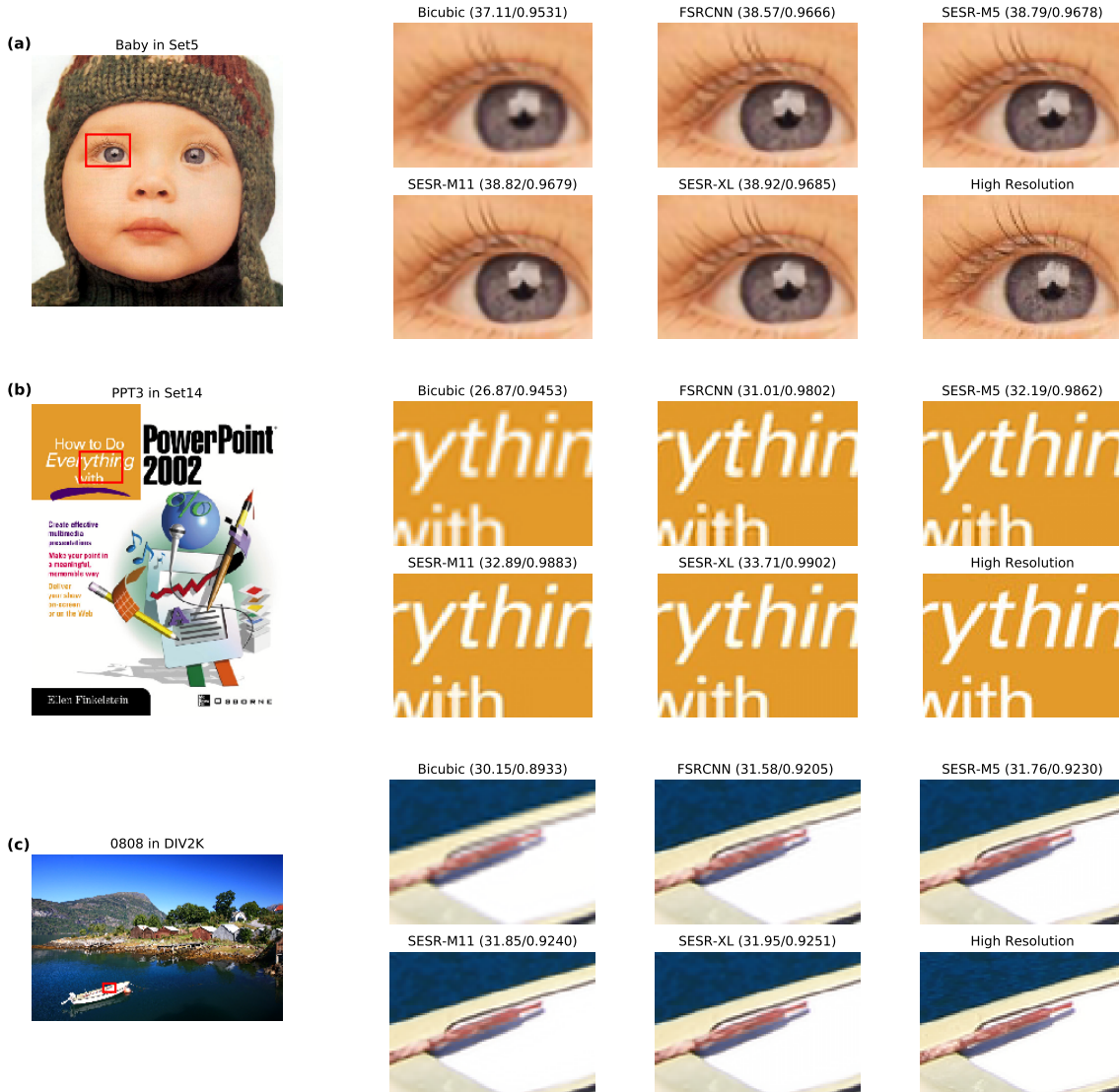


Figure 4. Qualitative comparison on $\times 2$ SISR. SESR-M5 shows significantly better image quality while needing $2\times$ fewer MACs than FSRCNN. SESR-M11, which has similar MACs as FSRCNN, yields even better results. Numbers in parenthesis indicate PSNR/SSIM.

Comparison against ExpandNets and the Effect of Short Residuals over 3×3 Linear Blocks. Recall that, similar to our work, ExpandNets [11] proposed decomposing a single $k \times k$ convolution into an overparameterized $k \times k$ convolution and a 1×1 convolution for image classification. In contrast, we further have a short residual on top of our 3×3 linear block that we collapse into convolution weights using Algorithm 2. We empirically found that these short residuals are essential for training such overparameterized networks for SISR tasks. To quantify this, we trained the SESR-M11 model using the exact same setup (e.g., learning rate, optimizer, etc.), but without the short residuals over 3×3 linear blocks (i.e., long blue and black residuals in Fig. 2(a) still exist). That is, this network is trained exactly using the procedure described by ExpandNets [11]. When

trained in this fashion, the model converged to 33.65dB DIV2K validation PSNR and did not improve further. This shows that the short residuals in our work are critical to obtain high accuracy on SISR tasks.

Effect of Linear Blocks. Next, we train the SESR-M11 architecture with both long and short residuals shown in Fig. 2(a) but without the linear blocks (i.e., only single convolutions are used throughout the network). This model converged to 35.25dB on DIV2K validation set. In contrast, the SESR-M11 with linear blocks achieves 35.45dB. Hence, linear blocks significantly improve the accuracy.

ReLU vs. PReLU and Input-to-Output Residual. Next, we replace all PReLU activations with ReLU activations in SESR-M11 network and also remove the long input-to-

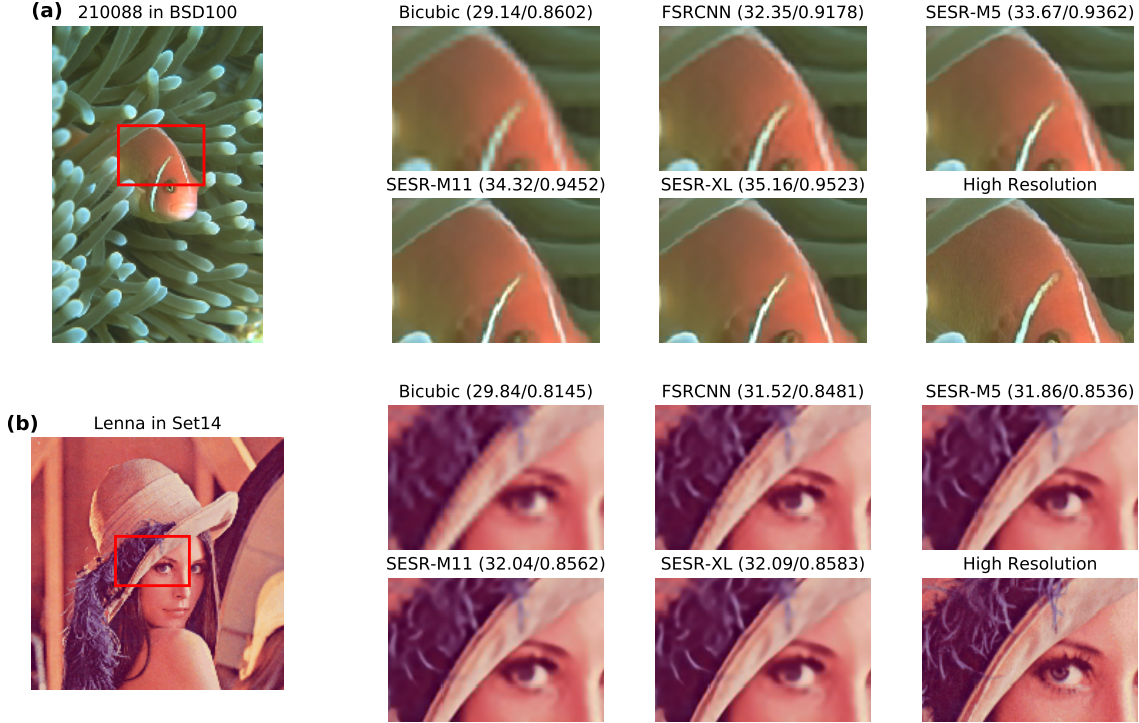


Figure 5. Qualitative comparison on $\times 4$ SISR. Both SESR-M5 and SESR-M11 require significantly fewer MACs than FSRCNN and yield better image quality (e.g., better edges, no unwanted halo, *etc.*). Numbers in parenthesis indicate PSNR/SSIM.

output residual (see long, black residual in Fig. 2(a)). Both of these changes can further improve hardware efficiency of SESR and this model will be used in the next section to show (simulated) hardware performance results on a commercial Arm Ethos-N78 mobile-NPU. This network loses only about 0.1dB PSNR on DIV2K validation dataset (*i.e.*, it achieves 35.35dB). Hence, this variant of SESR still significantly outperforms other similar sized networks like FSRCNN [9].

4.5. Hardware Performance Results

We now use the performance estimator for Arm Ethos-N78 NPU to simulate the hardware performance of different models running 1080p to 4K ($\times 2$) and 1080p to 8K ($\times 4$) SISR. Table 3 first shows MACs, DRAM Usage, Runtime and FPS for FSRCNN [9] and SESR-M5³ when converting a 1080p image to 4K resolution. As evident, even though SESR-M5 has $2\times$ fewer MACs than FSRCNN, the runtime is improved by $6.15\times$. This is because the hardware performance is guided not just by MACs but also the memory bandwidth⁴. The memory bandwidth for SISR tasks is heavily dependent on the sizes of activations. For FSRCNN,

³As mentioned, for hardware efficiency, we replace PReLU with ReLU in both SESR-M5 and FSRCNN, and also removed the input-to-output residual in SESR-M5. Again, both networks lose minimal PSNR (0.1dB).

⁴If data is not available to MAC units, they cannot perform the compute. Hence, both memory usage and MACs are important for efficiency.

CNN, the size of the largest activation tensor is $H \times W \times 56$, whereas for SESR-M5, it is $H \times W \times 16$, where $H \times W$ are the dimensions of low-resolution input. That is, SESR-M5's largest tensor is $3.5\times$ smaller than that of FSRCNN. We see that the DRAM use is correspondingly $2\times$ smaller in SESR-M5 than FSRCNN. This results in an overall $6.15\times$ better runtime. This shows the challenges of running real-world SISR on constrained devices and how SESR significantly outperforms FSRCNN.

Further optimizations to get up to $8\times$ better runtime.

As mentioned, DRAM usage for SISR application is naturally very high due to large input images (e.g., a 1080p input has 1920×1080 dimensions). To further accelerate the inference, the input can be broken down into tiles so that the DRAM traffic is minimized. As a proof-of-concept of this optimization, we divide a 1080p image into tiles of 400×300 and perform a $400 \times 300 \rightarrow 800 \times 600$ SISR. The performance numbers for this tile are given in Table 3. Clearly, we need to do this inference at least $(1920/400) \times (1080/300) = 17.28$ times to cover the entire input image. Hence, total inference time is given by (Performance for one tile $\times 17.28$) which comes out to about 21.77ms or ≈ 46 FPS (nearly $8\times$ faster than FSRCNN: 6FPS vs. 46FPS). Note that, these are only approximate calculations. In the real-world, there will be (i) boundary

Table 3. Hardware Performance on Arm Ethos-N78 NPU

Model and Resolution	MACs	DRAM Use (MB)	Runtime (ms) /FPS	Improvement (Runtime)
FSRCNN [9] ($\times 2$) 1080p \rightarrow 4K	54G	564.11	167.38/5.97	1 \times
SESR-M5 ($\times 2$) 1080p \rightarrow 4K	28G	282.03	27.22/36.73	6.15\times
SESR-M5 (Tiled, $\times 2$) 400 \times 300 \rightarrow 800 \times 600	1.62G	6.46	1.26/792.38	–
SESR-M5 ($\times 4$) 1080p \rightarrow 8K	38G	389.86	45.09/22.17	> 3.7\times
SESR-M5 (Tiled, $\times 4$) 400 \times 300 \rightarrow 1600 \times 1200	2.19G	9.84	2.12/471.69	–

overhead when tiling image to maintain the functional correctness, and (ii) other software overheads. However, since SESR-M5 network is not very deep, these overheads are not significant. This also brings us a little closer to 60FPS on a mobile-NPU when performing 1080p to 4K SISR.

Recall that, for $\times 4$ super resolution, SESR scales up better than FSRCNN in MACs. Hence, FSRCNN will achieve much less than 6FPS for 1080p to 8K SISR. In contrast, Table 3 shows that SESR-M5 achieves 22FPS which is at least 3.7 \times better than even $\times 2$ (1080p to 4K) FSRCNN’s 6FPS. Therefore, SESR will achieve significantly better performance than FSRCNN for 1080p to 8K SISR. Note that, we have estimated the final depth-to-space for our $\times 4$ network using [1080p to 4K] and [4K to 8K] (both using $\times 2$ SISR), instead of a one-shot $\times 4$ depth-to-space from 1080p to 8K. Hence, these numbers are still somewhat pessimistic and may be improved further using a one shot $\times 4$ depth-to-space operation. Finally, similar to the $\times 2$ SISR case above, with tiling, the 22FPS can be improved up to 27FPS (a runtime of $2.12 \times (1920/400) \times (1080/300)$ leads to 27FPS; see $\times 4$ tiling results in Table 3). Therefore, SESR enables 1080p to 4K and 1080p to 8K super resolution with significantly faster frame rates on real, commercial mobile-NPUs.

5. Conclusion

In this paper, we have proposed SESR, a new class of super-efficient super resolution networks that establish a new Pareto frontier on the quality-computation relationship for SISR problems. Our proposed networks are based on collapsible linear blocks that significantly improve the image quality while reducing the computational complexity. We have conducted detailed experiments across six datasets to demonstrate that SESR achieves similar or better image quality than state-of-the-art models while using $2\times$ to $330\times$ fewer MACs. This enables SESR to efficiently perform $\times 2$ (1080p to 4K) and $\times 4$ SISR (1080p to 8K) on resource constrained devices. To this end, we simulate hardware performance for 1080p to 4K ($\times 2$) and 1080p to 8K ($\times 4$) SISR on the Arm Ethos-N78 NPU. Our results demonstrate that SESR is significantly faster than prior art on mobile-NPUs.

References

- [1] Namhyuk Ahn, Byungkon Kang, and Kyung-Ah Sohn. Fast, accurate, and lightweight super-resolution with cascading residual network. In *Proceedings of the European Conference on Computer Vision (ECCV)*, pages 252–268, 2018. 1, 2, 5, 6
- [2] Saeed Anwar, Salman Khan, and Nick Barnes. A deep journey into super-resolution: A survey. *ACM Computing Surveys (CSUR)*, 53(3):1–34, 2020. 1
- [3] Arm. Ethos N78 Neural Processing Unit (NPU), 2020. Link: <https://www.arm.com/products/silicon-ip-cpu/ethos/ethos-n78>. Accessed: January 20, 2021. 1
- [4] Sanjeev Arora, Nadav Cohen, and Elad Hazan. On the optimization of deep networks: Implicit acceleration by over-parameterization. In Jennifer Dy and Andreas Krause, editors, *Proceedings of the 35th International Conference on Machine Learning*, volume 80 of *Proceedings of Machine Learning Research*, pages 244–253, Stockholm, Sweden, 10–15 Jul 2018. PMLR. 3
- [5] Andrew Burnes. NVIDIA DLSS-2.0, 2020. Link: <https://www.nvidia.com/en-us/geforce/news/nvidia-dlss-2-0-a-big-leap-in-ai-rendering/>. Accessed: January 15, 2021. 1
- [6] Xiangxiang Chu, Bo Zhang, Hailong Ma, Ruijun Xu, Jixiang Li, and Qingyuan Li. Fast, accurate and lightweight super-resolution with neural architecture search. *CoRR*, abs/1901.07261, 2019. 3
- [7] Xiangxiang Chu, Bo Zhang, and Ruijun Xu. Multi-objective reinforced evolution in mobile neural architecture search. In *European Conference on Computer Vision*, pages 99–113. Springer, 2020. 1, 5, 6
- [8] Xiaohan Ding, Yuchen Guo, Guiguang Ding, and Jungong Han. Acnet: Strengthening the kernel skeletons for powerful cnn via asymmetric convolution blocks. In *Proceedings of the IEEE/CVF International Conference on Computer Vision (ICCV)*, October 2019. 3
- [9] Chao Dong, Chen Change Loy, and Xiaoou Tang. Accelerating the super-resolution convolutional neural network. In *European conference on computer vision*, pages 391–407. Springer, 2016. 2, 4, 5, 6, 8, 9
- [10] Yuchen Fan, Honghui Shi, Jiahui Yu, Ding Liu, Wei Han, Haichao Yu, Zhangyang Wang, Xinchao Wang, and Thomas S Huang. Balanced two-stage residual networks for image super-resolution. In *Proceedings of the IEEE Conference on Computer Vision and Pattern Recognition Workshops*, pages 161–168, 2017. 5, 6
- [11] Shuxuan Guo, Jose M. Alvarez, and Mathieu Salzmann. Expandnets: Linear over-parameterization to train compact convolutional networks. In *Advances in Neural Information Processing Systems*, volume 33, pages 1298–1310, 2020. 3, 4, 7
- [12] Yong Guo, Yongsheng Luo, Zhenhao He, Jin Huang, and Jian Chen. Hierarchical neural architecture search for single image super-resolution. *IEEE Signal Processing Letters*, 27:1255–1259, 2020. 3

- [13] Geoffrey Hinton, Oriol Vinyals, and Jeff Dean. Distilling the knowledge in a neural network, 2015. [2](#)
- [14] Zheng Hui, Xiumei Wang, and Xinbo Gao. Fast and accurate single image super-resolution via information distillation network. In *Proceedings of the IEEE conference on computer vision and pattern recognition*, 2018. [2](#)
- [15] Jiwon Kim, Jung Kwon Lee, and Kyoung Mu Lee. Accurate image super-resolution using very deep convolutional networks. In *Proceedings of the IEEE conference on computer vision and pattern recognition*, pages 1646–1654, 2016. [5](#), [6](#)
- [16] J. Kim, J. K. Lee, and K. M. Lee. Accurate image super-resolution using very deep convolutional networks. In *2016 IEEE Conference on Computer Vision and Pattern Recognition (CVPR)*, pages 1646–1654, 2016. [2](#)
- [17] Jiwon Kim, Jung Kwon Lee, and Kyoung Mu Lee. Deeply-recursive convolutional network for image super-resolution. In *Proceedings of the IEEE conference on computer vision and pattern recognition*, 2016. [2](#)
- [18] Wei-Sheng Lai, Jia-Bin Huang, Narendra Ahuja, and Ming-Hsuan Yang. Deep laplacian pyramid networks for fast and accurate super-resolution. In *Proceedings of the IEEE conference on computer vision and pattern recognition*, pages 624–632, 2017. [6](#)
- [19] Christian Ledig, Lucas Theis, Ferenc Huszár, Jose Caballero, Andrew Cunningham, Alejandro Acosta, Andrew Aitken, Alykhan Tejani, Johannes Totz, Zehan Wang, et al. Photo-realistic single image super-resolution using a generative adversarial network. In *Proceedings of the IEEE conference on computer vision and pattern recognition*, pages 4681–4690, 2017. [2](#)
- [20] Royson Lee, Łukasz Dudziak, Mohamed Abdelfattah, Stylianos I Venieris, Hyeji Kim, Hongkai Wen, and Nicholas D Lane. Journey towards tiny perceptual super-resolution. In *European Conference on Computer Vision*, pages 85–102. Springer, 2020. [1](#), [2](#), [3](#), [4](#), [5](#), [6](#)
- [21] Xin Liu, Yuang Li, Josh Fromm, Yuntao Wang, Ziheng Jiang, Alex Mariakakis, and Shwetak N. Patel. Splitsr: An end-to-end approach to super-resolution on mobile devices. *CoRR*, abs/2101.07996, 2021. [2](#)
- [22] Xiaotong Luo, Yuan Xie, Yulun Zhang, Yanyun Qu, Cuihua Li, and Yun Fu. Latticenet: Towards lightweight image super-resolution with lattice block. In *European Conference on Computer Vision (ECCV)*, 2020. [2](#)
- [23] Abdul Muqeet, Jiwon Hwang, Subin Yang, Jung Heum Kang, Yongwoo Kim, and Sung-Ho Bae. Multi-attention based ultra lightweight image super-resolution. In *European Conference on Computer Vision (ECCV) 2020 Workshops*, 2020. [2](#)
- [24] Ying Nie, Kai Han, Zhenhua Liu, An Xiao, Yiping Deng, Chunjing Xu, and Yunhe Wang. Ghostsr: Learning ghost features for efficient image super-resolution. *CoRR*, abs/2101.08525, 2021. [2](#)
- [25] Mark Sandler, Andrew Howard, Menglong Zhu, Andrey Zhmoginov, and Liang-Chieh Chen. Mobilenetv2: Inverted residuals and linear bottlenecks, 2019. [3](#)
- [26] Wenzhe Shi, Jose Caballero, Ferenc Huszár, Johannes Totz, Andrew P Aitken, Rob Bishop, Daniel Rueckert, and Zehan Wang. Real-time single image and video super-resolution using an efficient sub-pixel convolutional neural network. In *Proceedings of the IEEE conference on computer vision and pattern recognition*, pages 1874–1883, 2016. [4](#)
- [27] Dehua Song, Chang Xu, Xu Jia, Yiyi Chen, Chunjing Xu, and Yunhe Wang. Efficient residual dense block search for image super-resolution. In *The Thirty-Fourth AAAI Conference on Artificial Intelligence*, 2020. [3](#)
- [28] Ying Tai, Jian Yang, and Xiaoming Liu. Image super-resolution via deep recursive residual network. In *Proceedings of the IEEE conference on computer vision and pattern recognition*, 2017. [2](#)
- [29] Ying Tai, Jian Yang, Xiaoming Liu, and Chunyan Xu. Memnet: A persistent memory network for image restoration. In *In Proceeding of International Conference on Computer Vision*, Venice, Italy, October 2017. [2](#)
- [30] Xuehui Wang, Qing Wang, Yuzhi Zhao, Junchi Yan, Lei Fan, and Long Chen. Lightweight single-image super-resolution network with attentive auxiliary feature learning. In *Proceedings of the Asian Conference on Computer Vision (ACCV)*, November 2020. [2](#)
- [31] Xintao Wang, Ke Yu, Shixiang Wu, Jinjin Gu, Yihao Liu, Chao Dong, Yu Qiao, and Chen Change Loy. Esrgan: Enhanced super-resolution generative adversarial networks. In *Proceedings of the European Conference on Computer Vision (ECCV) Workshops*, pages 0–0, 2018. [2](#)
- [32] Felix Wu, Amauri H. Souza Jr., Tianyi Zhang, Christopher Fifty, Tao Yu, and Kilian Q. Weinberger. Simplifying Graph Convolutional Networks. In *Proceedings of the 36th International Conference on Machine Learning*, pages 6861–6871. PMLR, 2019. [3](#)
- [33] Yan Wu, Zhiwu Huang, Suryansh Kumar, Rhea Sanjay Sukthankar, Radu Timofte, and Luc Van Gool. Trilevel neural architecture search for efficient single image super-resolution. *CoRR*, abs/2101.06658, 2021. [3](#)
- [34] Lei Xiao, Salah Nouri, Matt Chapman, Alexander Fix, Douglas Lanman, and Anton Kaplanyan. Neural supersampling for real-time rendering. *ACM Transactions on Graphics (TOG)*, 39(4):142–1, 2020. [1](#)
- [35] Yulun Zhang, Kunpeng Li, Kai Li, Lichen Wang, Bineng Zhong, and Yun Fu. Image super-resolution using very deep residual channel attention networks. In *European Conference on Computer Vision (ECCV)*, 2018. [2](#)
- [36] Yulun Zhang, Yapeng Tian, Yu Kong, Bineng Zhong, and Yun Fu. Residual dense network for image super-resolution. In *Proceedings of the IEEE Conference on Computer Vision and Pattern Recognition (CVPR)*, June 2018. [2](#)
- [37] Hengyuan Zhao, Xiangtao Kong, Jingwen He, Yu Qiao, and Chao Dong. Efficient image super-resolution using pixel attention, 2020. [2](#)
- [38] Barret Zoph, Vijay Vasudevan, Jonathon Shlens, and Quoc V. Le. Learning transferable architectures for scalable image recognition, 2018. [3](#)

Supplementary Results: Collapsible Linear Blocks for Super-Efficient Super Resolution

A. Additional Qualitative Results

Results for both $\times 2$ and $\times 4$ SISR are shown in Fig. 6 and Fig. 7 on the next two pages.

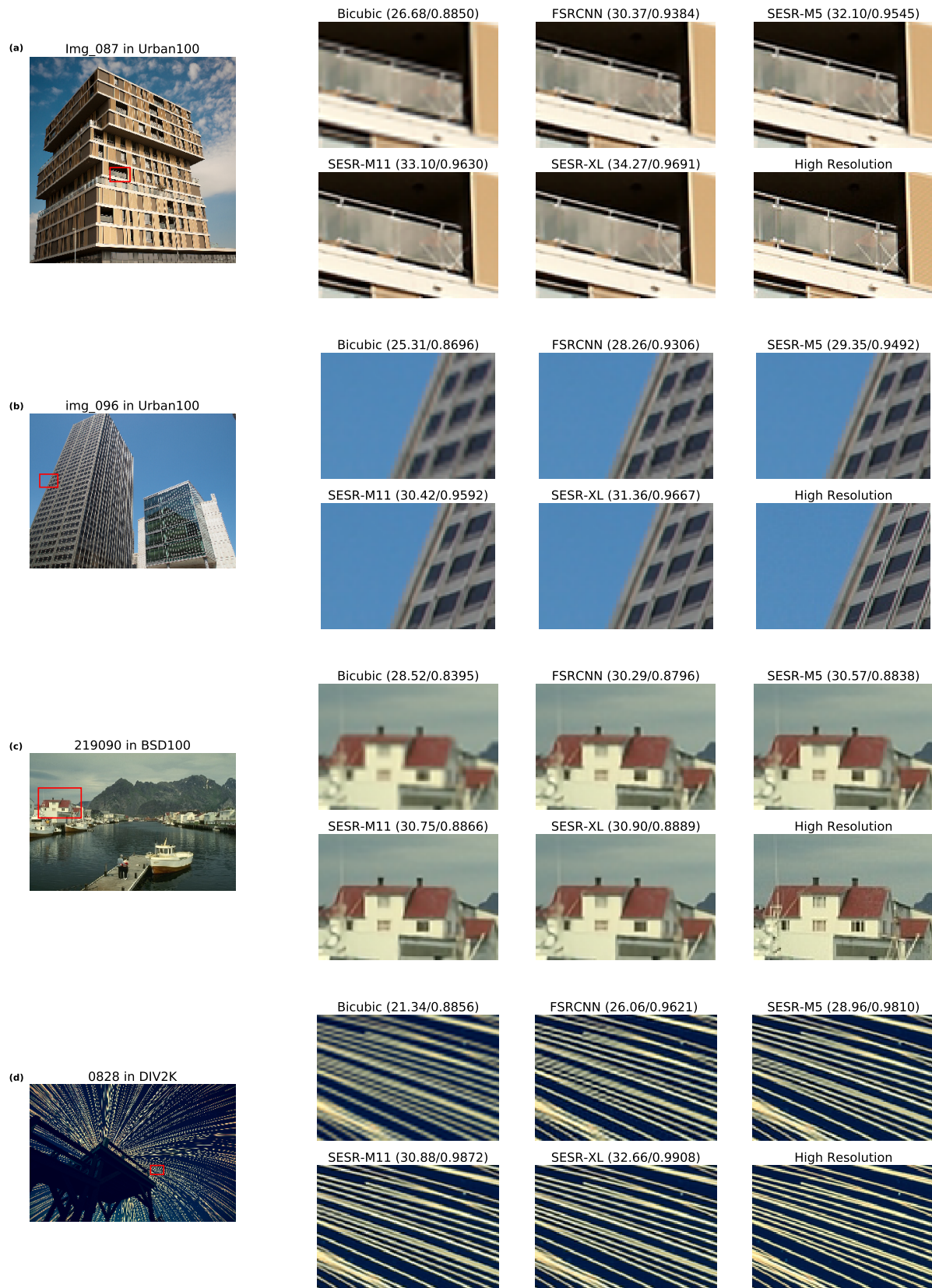


Figure 6. Additional Results: Qualitative comparison on $\times 2$ SISR. SESR-M5 shows much better image quality while needing $2\times$ fewer MACs than FSRCNN. SESR-M11 (similar MACs as FSRCNN) yields even better results. Numbers in parenthesis indicate PSNR/SSIM.

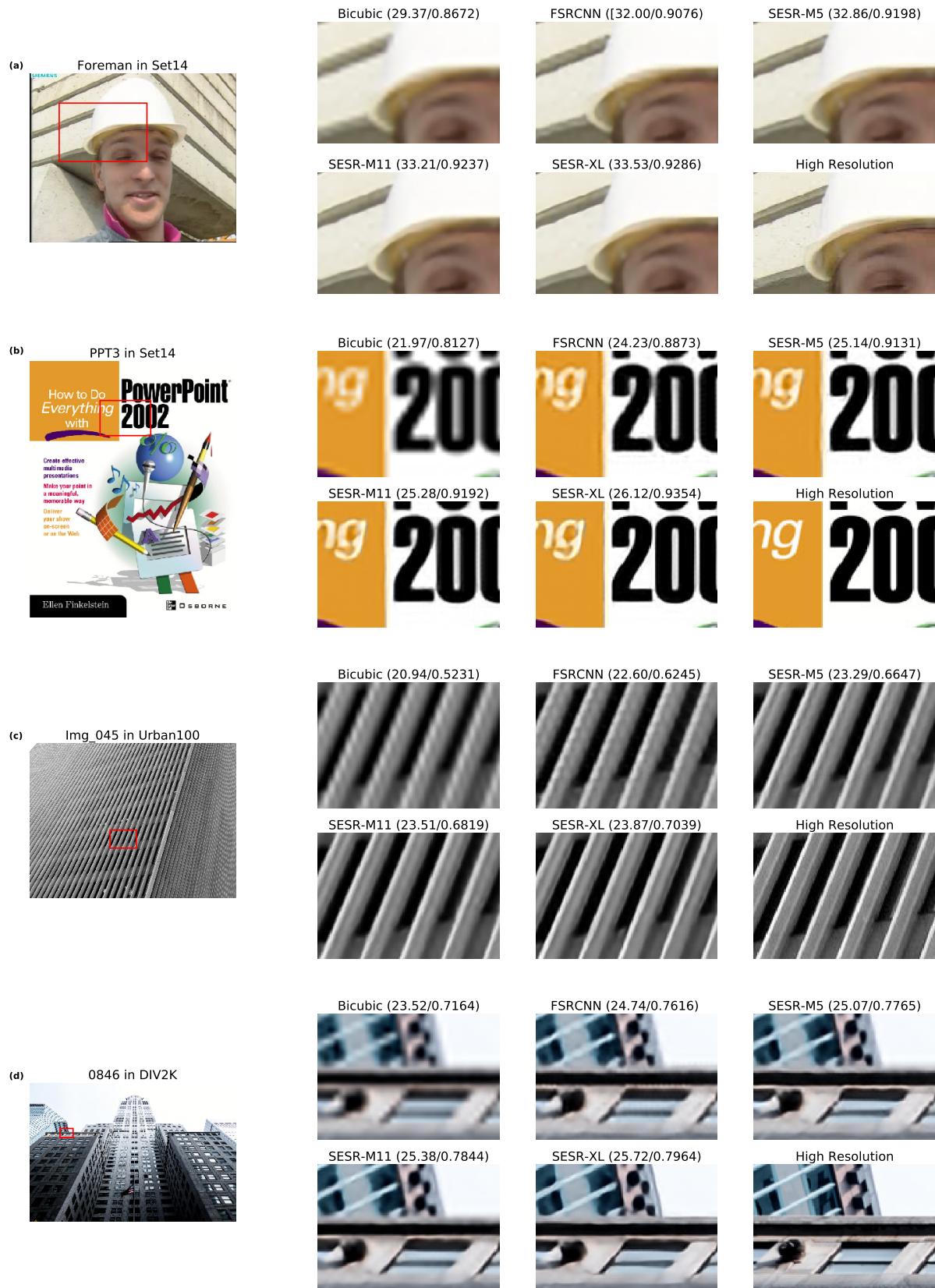


Figure 7. Additional Results: Qualitative comparison on $\times 4$ SISR. Both SESR-M5 and SESR-M11 require significantly fewer MACs than FSRCNN and yield better image quality (e.g., better edges, no unwanted halo, etc.). Numbers in parenthesis indicate PSNR/SSIM.